

To be published in Journal of the Optical Society of America B:

Title: Formation and interaction characteristics of two-component spatial weak-light soliton in a four-level double- λ type system

Authors: Yan She, Denglong Wang, Weixi Zhang, Zhangming He, and Jiannwen Ding

Accepted: 5 November 2009

Posted: 5 November 2009

Doc. ID: 115575

Formation and interaction characteristics of two-component spatial weak-light soliton in a four-level double- Λ type system

Yanchao She ¹, Denglong Wang ^{1,*}, Weixi Zhang ², Zhangming He ¹, Jianwen Ding ^{1,+}

¹ *Department of Physics & Institute for Nanophysics and Rare-earth Luminescence, Xiangtan University, Xiangtan 411105, China*

² *Department of Physics, Tongren University, Tongren 554300, China*

*Corresponding author: dlwang@xtu.edu.cn

+Corresponding author: jwding@xtu.edu.cn

By using the multiple-scale method, we study analytically the formation and stability of two-component spatial optical solitons in a cold, lifetime-broadened resonant four-level double- Λ type atomic system via electromagnetically induced transparency. It is shown that the stable two-component (1+1)-dimension spatial optical solitons with extremely weak-light intensity can occurred, which is different from the passive one with photorefractive and planar waveguides. Furthermore, the interaction characteristics between two solitons are studied by numerical simulations. We find that the collisional dynamics and the energy transfer of the two solitons are closely correlated with their relatives phase shift. Our results may provide a good idea to obtain the useful spatial optical soliton for application in optical soliton communications.

1. Introduction

Spatial optical soliton (SOS) is one type of localized optical beam forming in the nonlinear optical media when the effect of refractive nonlinearity can balance the diffraction effect of optical beam [1-2]. Based on the propagation characteristics of the solitons, the SOSs can make the beams propagate undistortedly over a long distance and remain unaffected after collision with each other. Such an interactional SOS may have potential applications in optical logic and switching. So, it has been investigated extensively by far [3-5]. However, most of the previous works on SOS are limited to conventional nonlinear mediums. In such mediums, a large nonlinear refractive index is always associated with large absorption. To avoid large absorption, people use optical fields far away from atomic resonances. However, this type of optical field only brings a very weak nonlinearity refractive index. If one would like to get obtain a larger nonlinearity to balance diffraction, highly intense light is needed. Therefore, it is hard to produce SOS at very low light intensities in the conventional nonlinear mediums.

To date, by means of the technique of electromagnetically induced transparency (EIT), the SOS has been realized at very low light intensities. It is mainly due to the fact that EIT can render an opaque medium transparency to a signal field with quantum interference effect induced by a coupling field, even when the signal field is tuned on to a very strong one-photon transition [6-8]. The wave propagation in the optical medium under EIT condition displays the significant enhancement of Kerr nonlinearity, which is

favorable to certain nonlinear optical processes under weak driving conditions [7-11]. Thus, the SOS can occur in a resonant atomic system [13-15]. In addition, the technique of EIT has also been used to produce high efficiency four-wave mixing [16-21], design quantum phase gates [22-24], and form temporal optical solitons with ultraslow propagating velocity [25-30].

As is known, one has understood the main characteristics of the SOS of one probe field [31-35]. However, there exist multiple probe fields in a single medium in reality, which are of interest in both fundamental physics and technical applications. For example, Li et al. [36] investigated the propagation properties of two probe fields in a four-state cascade-type system via EIT. They found that a two-component SOS can be produced under the condition of a rather low input power ($\sim mW$), quite different from the case of very high input power ($\sim kW$) in the conventional passive media. We here find that the SOSs can propagate stably in an ultracold four-level double- Λ type system. Meanwhile, we obtain that whether repulsive or attractive interaction, elastic or inelastic collision, and the energy transfer between the two SOSs are correlated with their phase shift. These behavior of SOS open possibilities for future applications in optical logic and switching devices.

2. The four-level double- Λ type system

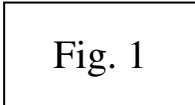


Fig. 1

The ultracold lifetime-broadened four-level double- Λ type gaseous atomic system, interacting with two weak probe fields and two strong control fields, is shown in Fig. 1. The probe fields (with center angular frequencies ω_p and ω_m) and the control fields (with center angular frequencies ω_a and ω_b) couple the transitions $|1\rangle \rightarrow |3\rangle$, $|1\rangle \rightarrow |4\rangle$ and $|2\rangle \rightarrow |3\rangle$, $|2\rangle \rightarrow |4\rangle$, respectively. The electric-field vector of the system can be written as $E = \sum_{l=a,b,p,m} \vec{e}_l \varepsilon_l \exp[i(k_l \cdot r - \omega_l t)] + c.c.$, where $\vec{e}_{p,m}$ ($\vec{e}_{a,b}$) are the unit vector denoting the polarization of the probe (control) fields, with the envelope $\varepsilon_{p,m}$ ($\varepsilon_{a,b}$). Here *c.c.* represents complex conjugate. In interaction picture, the material equations of motion

for atomic response reads

$$(i \frac{\partial}{\partial t} + d_2) A_2 + \Omega_a^* A_3 + \Omega_b^* A_4 = 0, \quad (1a)$$

$$(i \frac{\partial}{\partial t} + d_3) A_3 + \Omega_p A_1 + \Omega_a A_2 = 0, \quad (1b)$$

$$(i \frac{\partial}{\partial t} + d_4) A_4 + \Omega_m A_1 + \Omega_b A_2 = 0, \quad (1c)$$

$$|A_1|^2 + |A_2|^2 + |A_3|^2 + |A_4|^2 = 1, \quad (1d)$$

where A_j is the atomic probability amplitude. $\Omega_{p(m)} = \vec{e}_{p(m)} \cdot \vec{p}_{31(41)} \varepsilon_{p(m)} / \hbar$

($\Omega_{a(b)} = \vec{e}_{a(b)} \cdot \vec{p}_{32(42)} \varepsilon_{a(b)} / \hbar$) are the half Rabi frequencies corresponding to the probe (coupling) optical fields, with \vec{p}_{ij} being the electric dipole matrix element associated with the transition from $|j\rangle$ to $|i\rangle$. Here $d_j = \Delta_j + i\gamma_j$ ($j=2,3,4$), with $\Delta_{3(4)} = \omega_{p(m)} - (\omega_{3(4)} - \omega_1)$ and $\Delta_2 = \omega_p - \omega_a - (\omega_2 - \omega_1) = \omega_m - \omega_b - (\omega_2 - \omega_1)$. They are the one- and two-photon detuning between the states $|1\rangle \rightarrow |3\rangle$ ($|1\rangle \rightarrow |4\rangle$) and $|2\rangle \rightarrow |3\rangle$ ($|2\rangle \rightarrow |4\rangle$), respectively. γ_j is the decay rate of the state $|j\rangle$.

The equation of motion for $\Omega_{p(m)}$ can be obtained by the Maxwell equation

$$\nabla^2 \vec{E} - \frac{1}{c^2} \frac{\partial^2 \vec{E}}{\partial t^2} = \frac{1}{\varepsilon_0 c^2} \frac{\partial^2 \vec{P}}{\partial t^2}, \quad (2)$$

where $\vec{P} = N_a (\vec{p}_{14} c_1^* c_4 + \vec{p}_{13} c_1^* c_3 + \vec{p}_{24} c_2^* c_4 + \vec{p}_{23} c_2^* c_3 + c.c.)$. Under a slowly varying envelope approximation, equation (2) is turned into

$$i\left(\frac{\partial}{\partial z} + \frac{1}{c} \frac{\partial}{\partial t}\right)\Omega_p + \frac{c}{2\omega_p} \frac{\partial^2}{\partial x^2}\Omega_p + \kappa_{13} A_1^* A_3 = 0, \quad (3a)$$

$$i\left(\frac{\partial}{\partial z} + \frac{1}{c} \frac{\partial}{\partial t}\right)\Omega_m + \frac{c}{2\omega_m} \frac{\partial^2}{\partial x^2}\Omega_m + \kappa_{14} A_1^* A_4 = 0, \quad (3b)$$

where $\kappa_{13} = N_a |p_{13}|^2 \omega_p / (2\hbar \varepsilon_0 c)$ and $\kappa_{14} = N_a \omega_m |p_{14}|^2 / (2\varepsilon_0 \hbar c)$ are the propagation coefficients. N_a and c are the atomic density and light speed in vacuum, respectively. For simplicity, we assume that the coupling field is strong enough and unchanged, so that $\Omega_{a(b)}$ can be considered a constant here.

3. Asymptotic expansion and coupled nonlinear Schrödinger equations

Since equations (1) and (3) are nonintegrable, their soliton solutions can not be obtained directly. To get the propagation properties of nonlinear probe fields, we introduce multiple-scale perturbation theory [26, 28] to study the evolution of the probe optics in the four-level double- Λ type system. First, we make the following asymptotic expansions $A_1 = 1 + \sum_{j=2}^{\infty} \varepsilon^j A_1^{(j)}$, $A_l = \sum_{j=1}^{\infty} \varepsilon^j A_l^{(j)}$ ($l = 2, 3, 4$), $\Omega_{p(m)} = \sum_{j=1}^{\infty} \varepsilon^j \Omega_{p(m)}^{(j)}$, where ε is a small parameter characterizing the small population depletion of ground state. Then, we assume that $A_l^{(j)}$ ($l = 1, 2, 3, 4$), $\Omega_{p(m)}^{(j)}$ are functions of the multi-scale variables $t_l = \varepsilon^l t$ ($l = 0, 1$), $z_l = \varepsilon^l z$ ($l = 0, 1, 2$) and $x_l = \varepsilon x$. Substituting them into equations (1) and (3), we have a set of equations on $A_l^{(j)}$ and $\Omega_{p(m)}^{(j)}$, i.e.,

$$\left(i \frac{\partial}{\partial t_0} + d_2\right) A_2^{(j)} + \Omega_a^* A_3^{(j)} + \Omega_b^* A_4^{(j)} = \alpha^{(j)}, \quad (4a)$$

$$(i\frac{\partial}{\partial t_0} + d_3)A_3^{(j)} + \Omega_p^{(j)} + \Omega_a A_2^{(j)} = \beta^{(j)}, \quad (4b)$$

$$(i\frac{\partial}{\partial t_0} + d_4)A_4^{(j)} + \Omega_m^{(j)} + \Omega_b A_2^{(j)} = \gamma^{(j)}, \quad (4c)$$

$$i(\frac{\partial}{\partial z_0} + \frac{1}{c}\frac{\partial}{\partial t_0})\Omega_p^{(j)} + \kappa_{13}A_3^{(j)} = \delta^{(j)}, \quad (4d)$$

$$i(\frac{\partial}{\partial z_0} + \frac{1}{c}\frac{\partial}{\partial t_0})\Omega_m^{(j)} + \kappa_{14}A_4^{(j)} = \rho^{(j)}. \quad (4e)$$

The explicit expressions of $\alpha^{(l)}$, $\beta^{(l)}$, $\gamma^{(l)}$, $\delta^{(l)}$ and $\rho^{(l)}$ are omitted here for saving space.

The leading order is a pure linear problem. Ones may get

$$\Omega_p^{(1)} = F_+ e^{i[K_+(\omega)z_0 - \omega t_0]} + F_- e^{i[K_-(\omega)z_0 - \omega t_0]} = F_+ e^{i\theta_+} + F_- e^{i\theta_-}, \quad (5a)$$

$$\Omega_m^{(1)} = \frac{1}{\kappa_{13}\Omega_a\Omega_b^*} G_+ F_+ e^{i\theta_+} + \frac{1}{\kappa_{13}\Omega_a\Omega_b^*} G_- F_- e^{i\theta_-}, \quad (5b)$$

$$A_2^{(1)} = -\frac{1}{\Omega_a} H_+ F_+ e^{i\theta_+} - \frac{1}{\Omega_a} H_- F_- e^{i\theta_-}, \quad (5c)$$

$$A_3^{(1)} = \frac{1}{\kappa_{13}} (K_+ - \frac{\omega}{c}) F_+ e^{i\theta_+} + \frac{1}{\kappa_{13}} (K_- - \frac{\omega}{c}) F_- e^{i\theta_-}, \quad (5d)$$

$$A_4^{(1)} = \frac{1}{\kappa_{13}\kappa_{14}\Omega_a\Omega_b^*} (K_+ - \frac{\omega}{c}) G_+ F_+ e^{i\theta_+} + \frac{1}{\kappa_{13}\kappa_{14}\Omega_a\Omega_b^*} (K_- - \frac{\omega}{c}) G_- F_- e^{i\theta_-}, \quad (5e)$$

where $K_{\pm}(\omega) = \omega/c + [(\kappa_{13}D_b + \kappa_{14}D_a) \pm \sqrt{(\kappa_{13}D_b - \kappa_{14}D_a)^2 + 4\kappa_{14}\kappa_{13}|\Omega_a|^2|\Omega_b|^2}]/2D$,

$G_{\pm} = D(K_{\pm} - \omega/c) + \kappa_{13}D_b$, $H_{\pm} = (\omega + d_3)(K_{\pm} - \omega/c)/\kappa_{13} + 1$, $D_a = |\Omega_a|^2 - (\omega + d_2)(\omega + d_3)$

$D_b = |\Omega_b|^2 - (\omega + d_2)(\omega + d_4)$ and $D = |\Omega_a|^2(\omega + d_4) + |\Omega_b|^2(\omega + d_3) - (\omega + d_2)(\omega + d_3)(\omega + d_4)$.

And here F_{\pm} are envelope functions depending on the slow variables z_j ($j=1,2$)

and x_1 . For simplicity, in the following discussion we use the notation

$A_l^{(1)} = J_{0l+} F_+ e^{i\theta_+} + J_{0l-} F_- e^{i\theta_-}$ ($l=2,3,4$), where $J_{0l\pm}$ can be obtained by the

expressions (6) directly. In most operation conditions, $K_{\pm}(\omega)$ can be expanded as Taylor

Fig. 2

expansion around the center frequency of the probe field, i.e. $\omega = 0$. We have

$$K = K_{\pm}(\omega) = K_{\pm}(0) + K_{\pm}'\omega + K_{\pm}''\omega^2 + \dots \quad (6)$$

where $K_{\pm}(0) = \phi_{\pm} + i\alpha_{\pm}/2$ describe the linear absorption coefficient α_{\pm} and phase shift ϕ per unit length of the probe field. Usually, the absorptions of two component of probe field are different in the system. That is to say, there is a strong absorption to one component while a weak absorption to the other one in the system. When the probe field comes into the system, the former will be depleted. In this case, there may occur a single-component spatial optical soliton. Under the conditions that the parameters are chosen appropriately, however, there may exhibit weak absorption to the both components of the probe field. Figure 2 shows that the absorption coefficient α_{\pm} change with the Rabi frequency of control field Ω_a . We find that the both absorption coefficient α_{\pm} rapidly decrease with the increasing of the intensity of the control field Ω_a . It means that there exist parameter regimes in which the absorptions of the two components of the probe field can be almost suppressed simultaneously. These results are from the contribution of the control field Ω_a under an appropriate condition.

For the second order, a divergence-free solution requires

$$i\left(\frac{\partial}{\partial z_1} + \frac{1}{v_{g\pm}} \frac{\partial}{\partial t_1}\right)F_{\pm} = 0, \quad (7)$$

where $v_{g\pm} = (\partial K_{\pm} / \partial \omega)^{-1}$ is the group velocity of the wave envelope F_{\pm} .

Similarly, the third order yields the equation for F_{\pm} . Combining equation (6) and (7) and making transformation $t_l = \varepsilon^l t$ ($l=0,1$), $z_l = \varepsilon^l z$ ($l=0,1,2$) and $x_l = \varepsilon x$, we obtain

$$i\frac{\partial U_+}{\partial z} + iR\frac{\partial U_+}{\partial \tau} + K_{2+}\frac{\partial^2 U_+}{\partial \tau^2} + M_+\frac{\partial^2 U_+}{\partial x^2} + (N_{11}|U_+|^2 + N_{12}|U_-|^2)U_+ = 0, \quad (8a)$$

$$i\frac{\partial U_-}{\partial z} + iR\frac{\partial U_-}{\partial \tau} + K_{2-}\frac{\partial^2 U_-}{\partial \tau^2} + M_-\frac{\partial^2 U_-}{\partial x^2} + (N_{21}|U_+|^2 + N_{22}|U_-|^2)U_- = 0, \quad (8b)$$

where $U_{\pm} = \varepsilon F_{\pm}$, $\tau = t - z/v_g$, $R = -1/v_g$, $v_g = 2v_{g+}v_{g-}/(v_{g+} + v_{g-})$, $K_{2\pm} = \partial^2 K_{\pm}/\partial \omega^2$, $M_{\pm} = (I_{\pm}c/2\omega_p + G_{\pm}c/2\omega_m)/(G_{\pm} - I_{\pm})$, $I_{\pm} = (K_{\pm} - \omega/c)D - \kappa_{14}D_a$, $N_{11(22)} = \frac{1}{2}(K_{\pm} - \omega/c)J_{2\pm}$, and $N_{12(21)} = \frac{1}{2}(K_{\pm} - \omega/c)J_{2\mp}$. Obviously, equation (8) is the coupled Ginzburg-Landau

equations with complex coefficients and hence generally do not allow soliton solutions.

If, however, its parameters are chosen appropriately, ones may obtain its soliton solution. Moreover, when the imaginary parts of the coefficients can be much smaller

than the real parts (in the case of EIT), equation (8) can be reduced to couple nonlinear

Schrödinger (CNLS) equations. Here, the coefficients R , $K_{2\pm}$, M_{\pm} , $N_{11(22)}$, $N_{12(21)}$

describe the group velocity mismatch, dispersion, the spatial walk-off, self-phase

modulation (SPM) and cross-phase modulation (CPM) effects of the system,

respectively.

4. Coupled spatial soliton solutions and their stability

We now consider a steady state propagation regime of the soliton. As discussed in Ref. [36], the probe-field envelopes have such large enough temporal widths that their time evolution can be neglected. So the time-derivative terms in the equation (8) vanish.

Based on this idea, equation (8) may be rewritten as

$$i \frac{\partial v_+}{\partial \xi} + d_{1F} \frac{\partial^2 v_+}{\partial X^2} + (\beta_{11} |v_+|^2 + \beta_{12} |v_-|^2) v_+ = 0, \quad (9a)$$

$$i \frac{\partial v_-}{\partial \xi} + d_{2F} \frac{\partial^2 v_-}{\partial X^2} + (\beta_{21} |v_+|^2 + \beta_{22} |v_-|^2) v_- = 0, \quad (9b)$$

where the dimensionless variables $v_{\pm} = U_{\pm} / W_0$, $X = x / R_x$, $\xi = z / L_F$, $d_{1F} = M_+ / |M_-|$, $d_{2F} = M_- / |M_-|$, $\beta_{11} = N_{11} / |N_{22}|$, $\beta_{12} = N_{12} / |N_{22}|$, $\beta_{21} = N_{21} / |N_{22}|$, and $\beta_{22} = N_{22} / |N_{22}|$. Here $L_F = R_x^2 / |M_-|$, $L_N = 1 / |N_{22} W_0^2|$ and R_x are the characteristic diffraction length, nonlinear length and the beam width in the x direction of the probe field, and $W_0 = (M_- / N_{22})^{1/2} / R_x$. Disregarding the small imaginary parts of the coefficients, four types of coupled soliton solutions [37-43] of equation (9) are given in the following.

The bright-bright soliton pair solution is

$$v_+ = \sqrt{2} p_0 \operatorname{sech}[A(X - B\xi)] \exp\left\{i\left[\frac{B}{2d_{1F}} X + \left(A^2 d_{1F} - \frac{B^2}{4d_{1F}}\right)\xi\right]\right\}, \quad (10a)$$

$$v_- = \sqrt{2} q_0 \operatorname{sech}[A(X - B\xi)] \exp\left\{i\left[\frac{B}{2d_{2F}} X + \left(A^2 d_{2F} - \frac{B^2}{4d_{2F}}\right)\xi\right]\right\}, \quad (10b)$$

when the parameters satisfy with the condition $d_{1F} \beta_{22} = d_{2F} \beta_{12}$. Here $q_0^2 = (A^2 d_{1F} - \beta_{11} p_0^2) / \beta_{12}$, with p_0 , A and B being arbitrary real constants.

A bright-dark soliton pair solution is

$$v_+ = \sqrt{2} p_0 \operatorname{sech}[A(X - B\xi)] \exp\left\{i\left[\frac{B}{2d_{1F}} X + \left(A^2 d_{1F} - 2\beta_{12} q_0^2 - \frac{B^2}{4d_{1F}}\right)\xi\right]\right\}, \quad (11a)$$

$$v_- = \sqrt{2} q_0 \tanh[A(X - B\xi)] \exp\left\{i\left[\frac{B}{2d_{2F}} X - 2\left(A^2 d_{2F} + \beta_{21} p_0^2 + \frac{B^2}{8d_{2F}}\right)\xi\right]\right\}, \quad (11b)$$

with $q_0^2 = -(A^2 d_{1F} - \beta_{11} p_0^2) / \beta_{12}$.

A dark-bright soliton pair solution reads

$$v_+ = \sqrt{2} p_0 \tanh[A(X - B\xi)] \exp\left\{i\left[\frac{B}{2d_{1F}} X - 2(A^2 d_{1F} + \beta_{12} q_0^2 + \frac{B^2}{8d_{1F}})\xi\right]\right\}, \quad (12a)$$

$$v_- = \sqrt{2} q_0 \operatorname{sech}[A(X - B\xi)] \exp\left\{i\left[\frac{B}{2d_{2F}} X + (A^2 d_{2F} - 2\beta_{21} p_0^2 - \frac{B^2}{4d_{2F}})\xi\right]\right\}, \quad (12b)$$

with $q_0^2 = (A^2 d_{1F} + \beta_{11} p_0^2) / \beta_{12}$.

Ones can also obtain the dark-dark soliton pair solution

$$v_+ = \sqrt{2} p_0 \tanh[A(X - B\xi)] \exp\left\{i\left[\frac{B}{2d_{1F}} X - 2(A^2 d_{1F} + \frac{B^2}{8d_{1F}})\xi\right]\right\}, \quad (13a)$$

$$v_- = \sqrt{2} q_0 \tanh[A(X - B\xi)] \exp\left\{i\left[\frac{B}{2d_{2F}} X - 2(A^2 d_{1F} + \frac{B^2}{8d_{2F}})\xi\right]\right\}, \quad (13b)$$

with $q_0^2 = -(A^2 d_{1F} + \beta_{11} p_0^2) / \beta_{12}$.

Due to the existence of two dispersion branches (i.e., K_+ and K_-) in this system, each probe field is broken into two solitons. As a matter of fact, the formation of SOS pairs is due to the balance between the beam diffraction and nonlinearity (i.e., SPM and CPM) effects. It is possible that there exist bright-bright, bright-dark, dark-dark, dark-bright soliton pairs in our present system [36, 44-45], when the SPM and CPM coefficients defined by equation (9) satisfy the relation $\beta_{11}\beta_{22} = \beta_{12}\beta_{21}$. This is very different from conventional systems (such as photorefractive and planar waveguides) for generating SOS, where usually only one type of soliton pair can be produced.

Subsequently, the stability of the SOSs is cross-checked. For ^{87}Rb atoms, the decay rates and the detuning are $\gamma_2 = 2.0 \times 10^6 \text{ s}^{-1}$, $\gamma_3 = 5\gamma_4 = 5.0 \times 10^7 \text{ s}^{-1}$, and $\Delta_2 = -2.5 \times 10^8 \text{ s}^{-1}$, $\Delta_3 = \Delta_4 = 1.5 \times 10^9 \text{ s}^{-1}$, respectively. The propagation coefficients are $\kappa_{13} = \kappa_{14} = 1.0 \times 10^{10} \text{ m}^{-1} \text{ s}^{-1}$. The Rabi frequencies, beam width and wavelength of the probe fields are chosen as $|\Omega_b| = 1.5|\Omega_a| = 1.5 \times 10^9 \text{ s}^{-1}$, $R_x = 20 \mu\text{m}$ and $\lambda_m = \lambda_p = 0.16 \mu\text{m}$, respectively. Based on these

parameters, we obtain $\beta_{11} = \beta_{12} = 1.0 - 0.03i$, $\beta_{21} = \beta_{22} = 1.0 - 0.02i$, $d_{1F} = d_{2F} = 0.8 - 0.06i$, and $L_F = L_N = 2.5 \times 10^{-3} m$. As the diffraction length L_F is equal to the nonlinear length L_N , it illustrates the diffraction effect, causing the beam spread, is balanced with the nonlinear effect. So, the probe beam becomes self-trapped at a very narrow width and form the SOS. Figure 3 shows the spatial distribution of probe field intensity $|\Omega_p / W_0|^2$ for the bright-bright soliton. We see that the amplitude and width of the wave-packet characterizing probe field intensity keep unchanged and without attenuation. This means the SOS can stably propagating along the ξ -direction.

Fig. 3

In addition, we calculate the peak input power \vec{P}_{\max} of the SOS by Poynting's vector, and obtain $\vec{P}_{\max} \approx 8.3 \times 10^{-2} mW$. This clearly shown that only very low input power is required for generating SOS when using a highly resonant atomic medium.

However, in the conventional non-resonant medium such as photorefractives and planar waveguides, the optical field is usually needed to reach a very high peak power ($\sim 10^2 kW$) in order to bring out the enough nonlinear effect for SOS formation [15, 46].

5. Interactional characteristics between two spatial optical solitons

As is mentioned above, stable (1+1)-dimensional two-component SOSs can occur in the four-level double- Λ type system. This provides a possibility to detect

interaction between two SOSs. Starting from equation (9), we numerically simulate the interactional phenomena of the SOSs by using the split step Fourier method. The initial condition consists of two Gaussian beams, which is chosen as $v_+(\xi=0) = (\sqrt{2}/2)\text{sech}(X-3.0)\exp(-iX) + \rho(\sqrt{2}/2)\text{sech}(X+3.0)\exp[i(X+\phi_1)]$ and $v_-(\xi=0) = (\sqrt{2}/2)\text{sech}(X-3.0)\exp(-iX) + (\sqrt{2}/2)\text{sech}(X+3.0)\exp[i(X+\phi_2)]$, where ρ and ϕ_1 (or ϕ_2) represent the initial relative amplitudes and phase shift of two SOSs, respectively.

Fig. 4

For a fixed value of v_- , we consider the effect of v_+ on the probe beam intensity. In view of this consideration, we plot the spatial distribution of the probe beam intensity in the Fig. 4. Figure 4 (a) shows the result of the interaction between two SOSs with the same phase ($\phi_1 = 0$). We find that the two SOSs approach, collide, and separate each other. The intensity in the central region of the collision increase sharply. In this case, there exists attractive interaction between the two SOSs, which is from their constructive interference. Such constructive interference leads to an increase of the refractive index and hence attracts more light to the centre area. Compared with the case of Fig. 4 (a), we draw the result of the interaction between two SOSs with initial phase shift $\phi_1 = \pi$ in Fig. 4 (b). One sees that the interaction between the two SOSs is repulsive, because the refractive index lowers in the central area of the collision. The main reason is that there appears destructive interference between the amplitude of the

SOSs when two SOSs overlap each other. Meanwhile, from the Figs. 4(a) and 4(b), we obtain that the amplitude and width of the two SOSs seldom change after collision. It means the collisions between them are almost elastic. This kind of interaction between two SOSs with no energy losses is favorable for undistorted propagation of the single in the optical soliton communications. In addition, the interactional phenomenon between two SOSs with the phase shift $\phi_1 = -\pi/2$ and $\phi_1 = \pi/2$ are depicted as Fig. 4(c) and 4(d). We see that one of the solitons leading in phase has partly enhanced in its amplitude, and the other one lagging in phase has disappeared nearly after collision. We may infer that the soliton lagging in phase transfers some energy to another leading one, and there exist an inelastic collision between two solitons. So the one lagging in phase loss its most energy and disappeared nearly and enhance the other one. Such a collision scenario shown in Fig. 4(c) and 4(d) may be viewed as an amplification process in which one of the solitons represents a signal (or is a data carrier) while the other soliton represents an energy reservoir (pump). The main virtue of this amplification process is that it does not require any external amplification medium, and therefore the amplification of the soliton does not induce any noise [47]. The similar results for the v_- component can be also obtained. Our results described above may have promising application in optical logic and switching devices.

6. Conclusion

To summary, we have investigated a scheme to generate the two-component spatial optical solitons in a cold, four-level double- Λ type atomic system. It is shown

that the absorption of two-component of the probe field can be almost suppressed due to the contribution of the control fields under appropriate conditions. Meanwhile, we obtained analytically the CNLS equations describing the spatial distribution of probe field by using the method of multiple-scale. In addition, we demonstrated that multiple coupled SOSs can be generated by using very low input light intensity and propagated stably.

Furthermore, by means of numerical simulations we studied the interaction characteristics between the two SOSs. It was shown that whether repulsive or attractive interaction, elastic or inelastic collision, and the energy transfer between the two SOSs are correlated with their phase shift. The collision between two SOSs is elastic when they are in phase or out of phase. While the inelastic collision appears between the two SOSs with phase shift $\phi_1 = -\pi/2$ or $\phi_1 = \pi/2$. In addition, there exhibit an energy transfer between the two SOSs with different phase and enhance the one leading in phase.

Acknowledgements

Project is supported by National Natural Science Foundation of China (No. 10674113), the Program for New Century Excellent Talents in University (No. NCET-06-0707), the Foundation for the Author of National Excellent Doctoral Dissertation of China (Grant No. 200726), and partially by Scientific Research Fund of Hunan Provincial Education Department (No. 06A071).

Reference

1. H. A. Haus and W. S. Wong, "Solitons in optical communications," *Rev. Mod. Phys.* **68**, 423-444 (1996).
2. Y. S. Kivshar and B. Luther-Davies, "Dark optical solitons: physics and applications," *Phys. Rep.* **298**, 81-197 (1998).
3. G. A. Swartzlander, D. R. Andersen, J. J. Regan, H. Yin, and A. E. Kaplan, "Spatial Dark-Soliton Stripes and Grids in Self-Defocusing Materials," *Phys. Rev. Lett.* **66**, 1583 (1991).
4. G. I. Stegeman and M. Segev, "Optical Spatial Solitons and Their Interactions: Universality and Diversity," *Science*, **286**, 1518-1523 (1999).
5. Y. S. Kivshar and G. I. Stegeman, "spatial optical solitons," *Opt. Photonics News* **13**, 59-63 (2002).
6. G. X. Huang, K. J. Jiang, M. G. Payne, and L. Deng, "Formation and propagation of coupled ultraslow optical soliton pairs in a cold three-state double- Λ system," *Phys. Rev. E* **73**, 056606 (2006).
7. M. Fleischhauer, A. Imamoglu, and J. P. Marangos, "Electromagnetically induced transparency: Optics in coherent media," *Rev. Mod. Phys.* **77**, 633-673 (2005).
8. S. E. Harris, "Electromagnetically induced transparency," *Phys. Today* **50**, 36-42 (1997).
9. L. Deng, M. Kozuma, E. W. Hagley, and M. G. Payne, "Opening Optical Four-Wave Mixing Channels with Giant Enhancement Using Ultraslow Pump Waves," *Phys. Rev. Lett.* **88**, 143902 (2002).
10. M. Xiao, Y. Q. Li, S. Z. Jin, and J. Gea-Banacloche, "Measurement of Dispersive

- Properties of Electromagnetically Induced Transparency in Rubidium Atoms,” *Phys. Rev. Lett.* **74**, 666 (1995).
11. H. Kang and Y. F. Zhu, “Observation of Large Kerr Nonlinearity at Low Light Intensities,” *Phys. Rev. Lett.* **91**, 093601 (2003).
 12. T. Hong, M. W. Jack, M. Yamashita, and T. Mukai, “Enhanced Kerr nonlinearity for self-action via atomic coherence in a four-level atomic system,” *Opt. Commun.* **214**, 371-380 (2002).
 13. T. Hong, “Spatial Weak-Light Solitons in an Electromagnetically Induced Nonlinear Waveguide,” *Phys. Rev. Lett.* **90**, 183901 (2003).
 14. H. Michinel, M. J. Paz-Alonso, and V. M. Perez-Garcia, “Turning Light into a Liquid via Atomic Coherence,” *Phys. Rev. Lett.* **96**, 023903 (2006).
 15. C. Hang, G. X. Huang, and L. Deng, “Stable high-dimensional spatial weak-light solitons in a resonant three-state atomic system,” *Phys. Rev. E* **74**, 046601 (2006).
 16. P. R. Hemmer, D. P. Katz, J. Donoghue, M. Cronin-Golomb, M. S. Shahriar, and P. Kumar, “Efficient low-intensity optical phase conjugation based on coherent population trapping in sodium,” *Opt. Lett.* **20**, 982-984 (1995).
 17. Y. Li, M. Xiao, “Enhancement of nondegenerate four-wave mixing based on electromagnetically induced transparency in rubidium atoms,” *Opt. Lett.* **21**, 1064-1066 (1996).
 18. M. M. Kash, V. A. Sautenkov, A. S. Zibrov, L. Hollberg, G. R. Welch, M. D. Lukin, Y. Rostovtsev, E. S. Fry, and M. O. Scully, “Ultraslow Group Velocity and Enhanced Nonlinear Optical Effects in a Coherently Driven Hot Atomic Gas,” *Phys. Rev. Lett.*

- 82**, 5229 (1999).
19. D. A. Braje, V. Bali, S. Goda, G. Y. Yin, and S. E. Harris, “Frequency Mixing Using Electromagnetically Induced Transparency in Cold Atoms,” *Phys. Rev. Lett.* **93** 183601 (2004).
 20. Y. Zhang, B. Anderson, and M. Xiao, “Efficient energy transfer between four-wave-mixing and six-wave-mixing processes via atomic coherence,” *Phys. Rev. A* **77**, 061801 (2008).
 21. Y. Du, Y. Zhang, C. Zuo, C. Li, Z. Nie, H. Zheng, M. Shi, R. Wang, J. Song, K. Lu, and M. Xiao, “Controlling four-wave mixing and six-wave mixing in a multi-Zeeman-sublevel atomic system with electromagnetically induced transparency,” *Phys. Rev. A* **79**, 063839 (2009)
 22. C. Ottaviani, D. Vitali, M. Artoni, F. Cataliotti, and P. Tombesi, “Polarization Qubit Phase Gate in Driven Atomic Media,” *Phys. Rev. Lett.* **90**, 197902 (2003).
 23. D. Petrosyan, “Towards deterministic optical quantum computation with coherently driven atomic ensembles,” *J. Opt. B.* **7**, S141-S151 (2005).
 24. C. Hang, Y. Li, L. Ma, and G. X. Huang, “Three-way entanglement and three-qubit phase gate based on a coherent six-level atomic system,” *Phys. Rev. A* **74**, 012319 (2006).
 25. Y. Wu, and L. Deng, “Ultraslow bright and dark optical solitons in a cold three-state medium,” *Opt. Lett.* **29**, 2064-2066 (2004).
 26. G. X. Huang, L. Deng, and M.G. Payne, “Dynamics of ultraslow optical solitons in a cold three-state atomic system,” *Phys. Rev. E* **72** 016617 (2005).

27. L. Deng, M. G. Payne, G. X. Huang, and E. W. Hagley, "Formation and propagation of matched and coupled ultraslow optical soliton pairs in a four-level double- Λ system," *Phys. Rev. E* **72**, 055601 (R) (2005).
28. G. X. Huang, K. J. Jiang, M. G. Payne, and L. Deng, "Formation and propagation of coupled ultraslow optical soliton pairs in a cold three-state double- Λ system," *Phys. Rev. E* **73**, 056606 (2006);
29. J. Wang, C. Hang, and G. Huang, "Weak-light gap solitons in a resonant three-level system," *Phys. Lett. A* **366**, 528 (2007).
30. W. X. Yang, J. M. Hou, and R. K. Lee, "Ultraslow bright and dark solitons in semiconductor quantum wells," *Phys. Rev. A* **77**, 033838 (2008)
31. R. R. Moseley, S. Shepherd, D. J. Fulton, B. D. Sinclair, and M. H. Dunn, "Spatial Consequences of Electromagnetically Induced Transparency: Observation of Electromagnetically Induced Focusing," *Phys. Rev. Lett.* **74**, 670 (1995).
32. C. Hang, V. V. Konotop, G. X. Huang, "Spatial solitons and instabilities of light beams in a three-level atomic medium with a standing-wave control field," *Phys. Rev. A* **79**, 033826 (2009).
33. H. Michinel, M. J. Paz-Alonso, and V. M. Perez-Garcia, "Turning Light into a Liquid via Atomic Coherence," *Phys. Rev. Lett.*, **96**, 023903 (2006).
34. X. Wu, X. T. Xie, and X. X. Yang, "Dark and bright vortex solitons in electromagnetically induced transparent media," *J. Phys. B* **39**, 3263-3273 (2006).
35. X. T. Xie, W. B. Li, and X. X. Yang, "Bright, dark, bistable bright, and vortex spatial-optical solitons in a cold three-state medium," *J. Opt. Soc. Am. B* **23**,

- 1609-1614 (2006).
36. H. J. Li, G. X. Huang, "Two-component spatial optical solitons in a four-state ladder system via electromagnetically induced transparency," *Phys. Lett. A* **372**, 4127-4134 (2008).
37. B. Hu, G. X. Huang, and M.G. Velarde, "Dynamics of coupled gap solitons in diatomic lattices with cubic and quartic nonlinearities," *Phys. Rev. E* **62**, 2827 (2000);
38. F. Lu, Q. Lin, W.H. Knox, and G. P. Agrawal, "Vector Soliton Fission," *Phys. Rev. Lett.* **93**, 183901 (2004);
39. Z. G. Chen, A. Bezryadina, and I. Makasyuk, "Observation of two-dimensional lattice vector solitons," *Opt. Lett.* **29**, 1656-1658 (2004).
40. C. R. Menyuk, "Stability of solitons in birefringent optical fibers. I: Equal propagation amplitudes," *Opt. Lett.* **12**, 614-616 (1987);
41. S. Trillo, S. Wabnitz, E. M. Wright, and G. I. Stegeman, "Optical solitary waves induced by cross-phase modulation," *Opt. Lett.* **13**, 871-873 (1988);
42. V. V. Afanasyev, Y. S. Kivshar, V. V. Konotop, and V. N. Serkin, "Dynamics of coupled dark and bright optical solitons," *Opt. Lett.* **14**, 805-807 (1989);
43. Y. S. Kivshar and S. K. Turitsyn, "Vector dark solitons," *Opt. Lett.* **18**, 337-339 (1993).
44. C. Hang and G. Huang, "Weak-light ultraslow vector solitons via electromagnetically induced transparency," *Phys. Rev. A* **77**, 033830 (2008).
45. L. G. Si, W. X. Yang, and X. X. Yang, "Ultraslow temporal vector optical solitons in a cold four-level tripod atomic system," *J. Opt. Soc. Am. B* **26**, 478-486 (2009).
46. J. S. Aitchison, A. M. Weiner, Y. Silberberg, M. K. Oliver, J. L. Jackel, D. E. Leaird, E.

M. Vogel, and P. W. E. Smith, "Observation of spatial optical solitons in a nonlinear glass waveguide," *Opt. Lett.* **15**, 471-473 (1990).

47. W. J. Liu, B. Tian, H. Q. Zhang, L. L. Li, and Y. S. Xue, "Soliton interaction in the higher-order nonlinear Schrödinger equation investigated with Hirota's bilinear method," *Phys. Rev. E* **77**, 066605 (2008).

Published by

OSA

Figure captions

Fig. 1 The lifetime-broadened four-level double- Λ type atomic system interact with two weak probe fields (of which center angular frequencies and Rabi frequencies are $\omega_{p(m)}$ and $\Omega_{p(m)}$) and two strong control fields (of which center angular frequencies and Rabi frequencies are $\omega_{a(b)}$ and $\Omega_{a(b)}$), respectively. Δ_j ($j=2,3,4$) is the detuning.

Fig. 2 The absorption coefficients α_{\pm} of two-component of the probe field versus Rabi frequency Ω_a , obtained with $|\Omega_b|=1.0\times 10^9 s^{-1}$. Other parameters of this system are $\kappa_{14}=2\kappa_{13}=2.0\times 10^{12} m^{-1} s^{-1}$, $\Delta_2=\Delta_3=1.0\times 10^8 s^{-1}$, $\Delta_4=2.0\times 10^8 s^{-1}$, $\gamma_3=\gamma_4=2.0\times 10^8 Hz$, $\gamma_2=2.0\times 10^7 Hz$.

Fig. 3 The space evolution of the relative probe field intensity $|\Omega_p|^2$ in the case of bright-bright soliton solution as a function of dimensionless diffraction width $X=x/R_x$ and propagation distance $\xi=z/L_F$ with $R_x=20\mu m$ and $L_F=2.5mm$. Other parameters are $\gamma_2=2.0\times 10^6 s^{-1}$, $\gamma_3=5\gamma_4=5.0\times 10^7 s^{-1}$, $\Delta_2=-2.5\times 10^8 s^{-1}$, $\Delta_3=\Delta_4=1.5\times 10^9 s^{-1}$, $\lambda_m=\lambda_p=0.16\mu m$, $\kappa_{13}=\kappa_{14}=1.0\times 10^{10} m^{-1} s^{-1}$, $|\Omega_b|=1.5|\Omega_c|=1.5\times 10^9 s^{-1}$, $A=1.0$, $B=0.1$, and $p_0=0.5$.

Fig. 4 The spatial distribution of $|\Omega_p|^2$ for the interactions between two-solitons with (a) $\rho=1.4$, $\phi_1=0$, (b) $\rho=1.4$, $\phi_1=\pi$, (c) $\rho=1.0$, $\phi_1=-\pi/2$, (d) $\rho=1.0$, $\phi_1=\pi/2$.

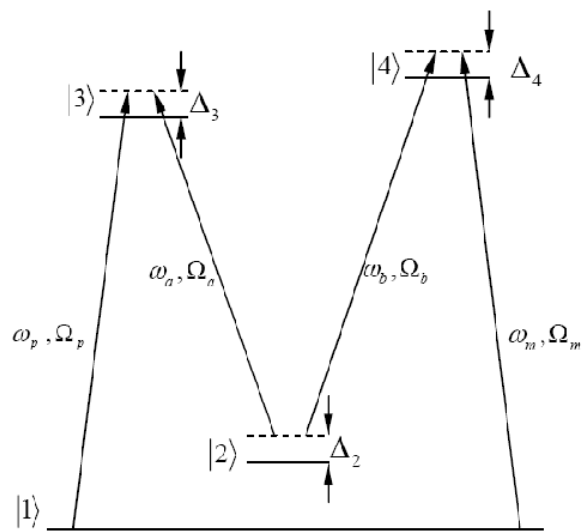


Fig. 1

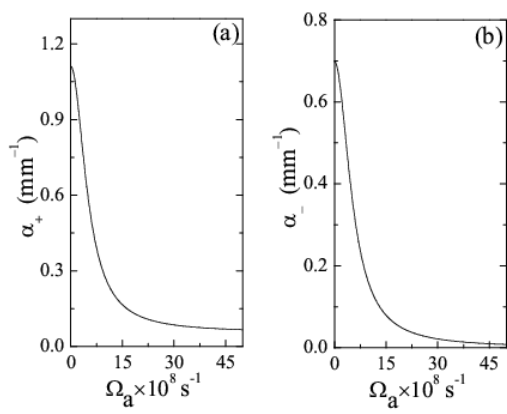


Fig. 2

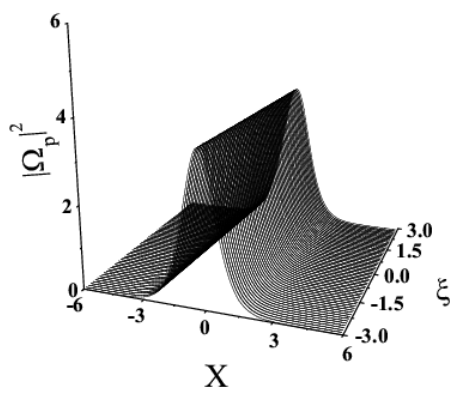


Fig. 3

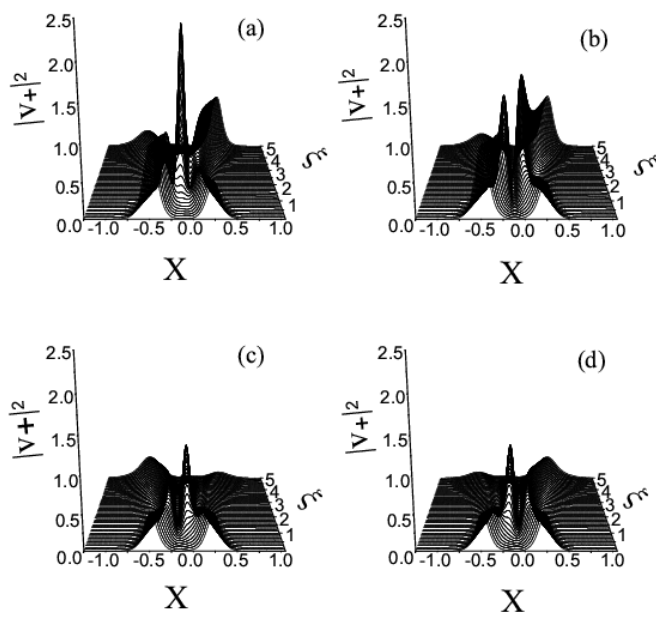


Fig. 4